Aleksandra SIKORA
KIELCE UNIVERSITY OF TECHNOLOGY, DIVISION OF ELECTRICAL ENGINEERING AND MEASUREMENT SYSTEMS
7 Tysiąclecia Państwa Polskiego Ave., 25-341 Kielce

Parameter comparison of fiber Bragg grating based optical wavelength discriminators

Abstract

Fiber Bragg gratings (FBGs) are widely used as temperature and strain measurement systems and in telecommunications systems. In order to simplify detecting the wavelength change (which is the output signal from FBB), fiber Bragg grating based optical wavelength discriminators can be used. In this paper, discriminators with apodized, chirped FBG cooperating with the identical grating of a sensor are considered. The analysis includes: the processing range (assuming the nonlinearity characteristic is less than 1%), the processing equation and the range of strain measurement. On the basis of simulation tests, there is discussed the influence of the following parameters: chirp value (Subsection 3.1), length (Subsection 3.2) and constant refractive index change averaged over the grating period (Subsection 3.3) of selected FBGs on the discriminator characteristic.

Keywords: fiber Bragg grain, FBG, chirped fiber Bragg grating, strain measurement.

1. Introduction

A fiber Bragg grating (FBG) is a part of optical fiber where the index of reflection experiences periodic modulation. When the broadband light is injected into the fiber, the grating reflects particular wavelengths, named the Bragg wavelengths λ_B [1]:

$$\lambda_B = 2n_{eff}\Lambda, \tag{1}$$

where n_{eff} if the effective refractive index inside the grating, Λ is the grating period.

The Bragg wavelength is changed by temperature and strain variation. The change caused by the axial strain is given by:

$$\Delta\lambda_B = (1 - p_e)\varepsilon\lambda_B, \tag{2}$$

where ε is the applied strain and p_e is the photoelastic coefficient.

In this paper, the apodized, chirped FBGs are considered. For this kind of grating, Eq. 1 can be written as:

$$\lambda_B(z) = 2n_{eff}(z)\Lambda(z), \tag{3}$$

where the parameters depend on z, and z is the distant along the length of the grating. Here, selected chirped FBGs have linear variation of the grating period:

$$\Lambda(z) = \Lambda_0 + \Lambda_l z, \tag{4}$$

where Λ_0 is the staring period, and Λ_l is the linear change along the grating. In this paper, the chip parameter is defined for Eqs. 3 and 4 as a wavelength shift factor $\frac{d\lambda}{dz}$.

The effective refractive index $n_{eff}(z)$ can be described by the following function:

$$n_{eff}(z) = n_0\left(1 + \overline{\delta n_{eff}}g(z)cos\left(\frac{2\pi}{\Lambda}z + \varphi(z)\right)\right), \tag{5}$$

where: n_0 is the mean value of the refractive index, $\overline{\delta n_{eff}}$ is the constant refractive index change averaged over the grating period, $g(z)$ is the apodization function, $\varphi(z)$ describes the grating chirp.

In the application of FBG, different features are required. The grating length is crucial when the FBG processes a dynamic strain [2], whereas in telecommunications, when the FBG is used as a narrowband optic filter, the slope of the power reflection coefficient is significant. The following part of the paper is focused on the influence of parameters of the used FBGs on the discriminator characteristic.

2. Operating principle and method of study

Signal detection from the FBG can be achieved by a FBG-based optical discriminator (Fig. 1). This system consists of a broadband source, a reference FBG, an optical circulator, a sensing FBG and an optical spectrum analyzer. The reference FBG, which is illuminated by the broadband source (terminals 1 and 2), reflects a part of the incident beam. The reflected beam is propagated by an optical circulator (terminals 2 and 3) to the sensing FGB. The sensing FBG reflects a part of the light, depending on the acting strain. The result is then propagated by the optical circulator (terminals 3 and 4) to the optical spectrum analyzer. In the presented circuit, the acting strain causes a change in the reflected spectrum for the sensing FBG.

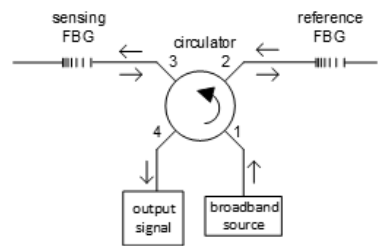

Fig. 1. The measuring circuit with the reference FBG as a discriminator

The optical power P_{out} is obtained from the expression [3]:

$$P_{out}(\Delta\lambda_B) = \int_{\lambda_1}^{\lambda_2} I(\lambda)R_r(\lambda)R_s(\lambda - \Delta\lambda_B)d\lambda, \tag{6}$$

where: $I(\lambda)$- spectral power density of the light source, $R_r(\lambda)$- response of the reference FBG, $R_s(\lambda)$ – response of the sensing FBG, $\Delta\lambda_B$ - change in the Bragg wavelength of sensing FBG caused by the measuring strain, λ_1 and λ_2 are the low and upper wavelength of source band. On the grounds of Eq. 6, the discriminators processing characteristic are calculated assuming the constant value of the spectral power density of the light source.

The responses ($R_r(\lambda)$ and $R_s(\lambda)$) of gratings, which are the power reflection coefficients for apodized, chirped FBGs, are calculated by the transfer matrix method [1, 4-6]. In this method, the initial non uniform grating is divided into a series of smaller length Δz uniform FBG increasing in the period. Each of this M-section is described by the transfer matrix T_m, where $m\epsilon(1, M)$. The whole structure of grating is described by multiplications of matrices:

$$T_{1..M} = T_1 \cdot T_2 \cdot \ldots T_M = \begin{bmatrix} t_{11} & t_{12} \\ t_{21} & t_{22} \end{bmatrix}, \tag{7}$$

where t_{11}, t_{12}, t_{21} and t_{22} are the results of a mathematical model of the FBG – a pair of coupled differential equations describing the interaction between the propagation and counter-propagation modes. Then the reflected spectrum is given by the equation:

$$R = \left|-\frac{t_{21}}{t_{22}}\right|^2. \tag{8}$$

3. Results of simulations

The processing characteristics of nine FBG-based discriminators with the identical sensing FBG and reference FBG were calculated. All the simulated gratings have the Bragg wavelength $\lambda_B = 1550$ nm. The results are divided into three sections: discriminators with the FBGs with the pairwise different chirp value (Subsection 3.1), with the pairwise different length L (Subsection 3.2) and the pairwise different constant refractive index change averaged over the grating period $\overline{\delta n_{eff}}$ (Subsection 3.3). The temperature dependence of the Bragg wavelength is omitted, the condition of constant temperature is established.

3.1. FBG-based optical discriminators with different chirp $\frac{d\lambda}{dz}$ value

The gratings parameters are presented in Table 1. The corresponding characteristics of the power reflection coefficient are presented in Fig. 2. The parameter FWHM is the width of the spectrum at half height.

Tab. 1. Parameters of selected FBGs: $L = 6$ mm , $\overline{\delta n_{eff}} = 5 \cdot 10^{-4}$, $n_{eff} = 1.45$.

No.	FWHM, nm	Chirp, nm/cm	Type of line
1	0.83	3	solid
2	1.17	2	dashed
3	1.61	1	dotted

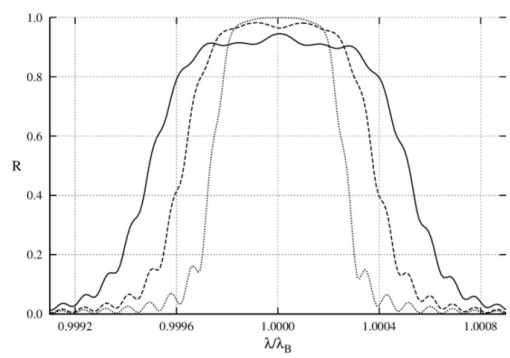

Fig. 2. Spectra of the power reflection coefficient for FBGs with different value of chirp. Solid line – grating number 1, dashed line – grating no. 2, dotted line- grating no. 3

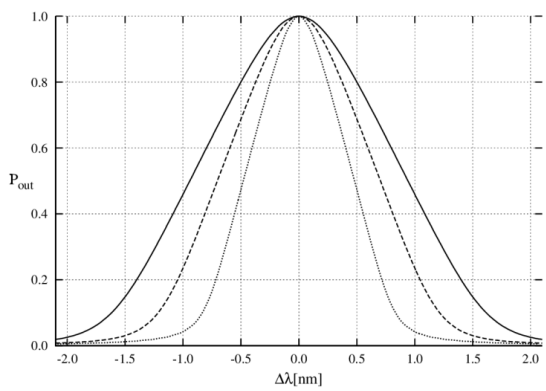

Fig. 3. The discriminator characteristics (P_{out} is in relative units). Solid line – for discriminator built with the two identical grating with parameters no. 1, dashed line – with parameters no. 2, dotted line – with parameters no. 3

Tab. 2. Comparison of the studied discriminator systems

No.	Processing range, nm	Processing equation	Type of line
1	0.495	$P_{out} = 1.29\Delta\lambda + 1.12$	dotted
2	0.705	$P_{out} = 0.90\Delta\lambda + 1.14$	dashed
3	0.930	$P_{out} = 0.68\Delta\lambda + 1.14$	solid

Fig. 3 shows the obtained discriminator characteristics. Table 2 presents the calculated processing range and processing equations under the assumption that the nonlinearity characteristic is less than 1%. The given processing equation is presented for a growing part of the characteristic.

For selected values of chirp: $1\frac{\text{nm}}{\text{cm}}$, $2\frac{\text{nm}}{\text{cm}}$ and $3\frac{\text{nm}}{\text{cm}}$ (and constant other parameters of the gratings), the processing ranges are 0.495 nm, 0.705 nm and 0.930 nm equivalent to 409με, 583 με and 769 με the range of strain measurement, respectively.

3.2. FBG-based optical discriminators with different length L of FBG

The parameters of selected gratings are listed in Table 3. The corresponding characteristics of the power reflection coefficient are presented in Fig. 4.

Tab. 3. Parameters of selected FBGs: $\frac{d\lambda}{dz} = 2\ \frac{\text{nm}}{\text{cm}}$, $\overline{\delta n_{eff}} = 5 \cdot 10^{-4}$, $n_{eff} = 1.45$

No.	FWHM, nm	L, mm	Type of line
4	1.02	5	solid
5	1.17	6	dashed
6	1.37	7	dotted

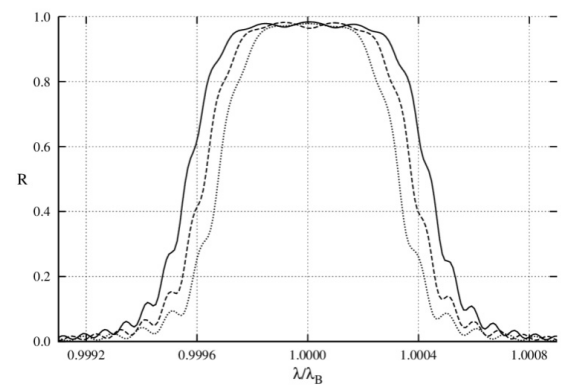

Fig. 4. Spectra of the power reflection coefficient for FBGs with different length L

The calculated discriminator characteristics are shown in Fig. 5 and the obtained results are presented in Table 4.

For selected values of the grating length: 6 mm, 7 mm and 8 mm (and constant other parameters of the gratings), the processing ranges are 0.555 nm, 0.705 nm and 0.855 nm equivalent to 459με, 583 με and 707 με the range of strain measurement, respectively.

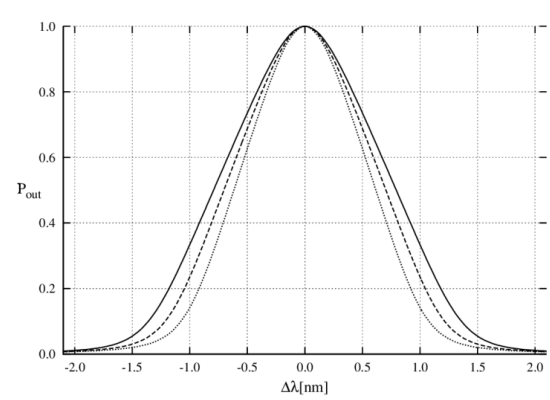

Fig. 5. The discriminator characteristics for gratings no. 4, 5 and 6

Tab. 4. Comparison of the studied discriminator systems

No.	Processing range, nm	Processing equation	Type of line
4	0.555	$P_{out} = 1.05\Delta\lambda + 1.15$	dotted
5	0.705	$P_{out} = 0.91\Delta\lambda + 1.14$	dashed
6	0.855	$P_{out} = 0.79\Delta\lambda + 1.13$	solid

3.3. FBG-based optical discriminators with different constant refractive index change $\overline{\delta n_{eff}}$

The parameters of selected gratings are listed in Table 5 and the corresponding characteristics of the power reflection coefficient are presented in Fig. 6. The calculated discriminator characteristics are shown in Fig. 7 and the obtained results are given in Table 6.

For selected values of the constant refractive index change averaged over the grating period $\overline{\delta n_{eff}}$: $3 \cdot 10^{-4}$, $4 \cdot 10^{-4}$ and $5 \cdot 10^{-4}$ (and constant other parameters of the gratings), the processing ranges are 0.510 nm, 0.585 nm and 0.705 nm equivalent to 422με, 484 με and 583 με the range of strain measurement, respectively.

Tab. 5. Parameters of selected FBGs: $L = 6$ mm , $\frac{d\lambda}{dz} = 2\ \frac{\text{nm}}{\text{cm}}$, $n_{eff} = 1.45$

No.	FWHM, nm	$\overline{\delta n_{eff}}\ 10^{-4}$	Type of line
7	0.99	3	dotted
8	1.07	4	dashed
9	1.12	5	solid

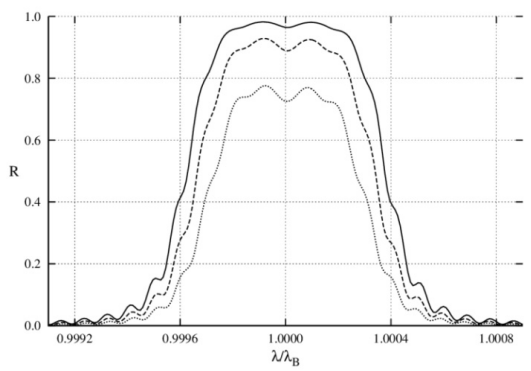

Fig. 6. Spectra of the power reflection coefficient for FBGs with different constant refractive index change averaged over the grating period $\overline{\delta n_{eff}}$

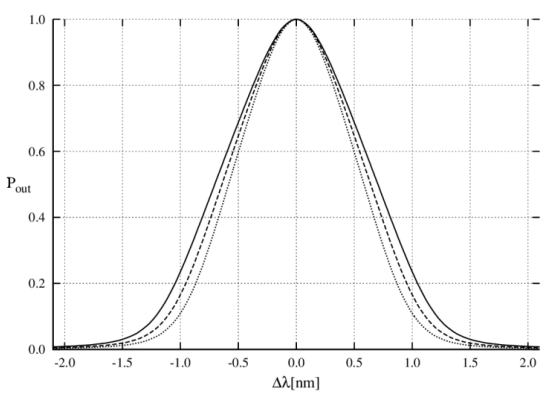

Fig. 7. The discriminator characteristics for gratings no. 7, 8 and 9

Tab. 6. Comparison of the studied discriminator systems

No.	Processing range, nm	Processing equation	Type of line
7	0.510	$P_{out} = 1.13\Delta\lambda + 1.16$	dotted
8	0.585	$P_{out} = 1.02\Delta\lambda + 1.15$	dashed
9	0.705	$P_{out} = 0.91\Delta\lambda + 1.14$	solid

4. Conclusions

For the purpose of measurement, the discriminator linear operating range is used. It arises from the reflected spectrum from gratings.

The analysis of the results showed that for the investigated gratings, the wider the reflected spectrum (the FWHM parameter), the wider the processing range and the measurement strain range. The pairwise replacement of the grating with a higher and higher chirp value (Subsection 3.1, in the range from 1 $\frac{\text{nm}}{\text{cm}}$ to 3 $\frac{\text{nm}}{\text{cm}}$, with the other parameters the same) in the simulated circuit extends the processing range by 0.435 nm (corresponding to extension 360 με in measured strain). In Subsection 3.2, replacing the grating with the increasing length L (in the range from 5 nm to 7 nm), resulted in extending the processing range by 0.3 nm (corresponding to the extension 360 με in the measured strain). In Subsection 3.3, replacing the grating with increasing the constant refractive index change averaged over the grating period $\overline{\delta n_{eff}}$ (in the range from $3 \cdot 10^{-4}$ to $5 \cdot 10^{-4}$) extends the processing range by 0.195 nm (corresponding to extension 161 με in the mesured strain).

The analysis provides a guide for selecting apodized, chirped fiber Bragg grating in the implementation of an optical wavelength discriminator.

5. References

[1] Othonos A., Kalli K.: Fiber Bragg Gratings. Fundamentals and Applications in Telecommunications and Sensing. Boston London, Artech House, 1999.

[2] Kaczmarek Z., Sikora A.: Influence of the length of a uniform fiber Bragg grating on the accuracy of measuring an impulsive strain, Optica Applicata, Vol. XXXVIII, No. 2, 2008.

[3] Jóźwik A., Kaczmarek C., Kaczmarek T., Kaczmarek Z.: Optical wavelength discriminator with an apodized uniform fiber Bragg grating. Proceedings of SPIE 5576, pp. 50–53, 2004.

[4] Dionisio R.P., Lima M. J., Da Rocha J. R. F., Pinto J. L., Teixeira A. J.: Numerical methods for fiber Bragg gratings. Proceedings of 5th Intern. Conf. on Transparent Optical Networks, Warsaw, Poland, pp. 185–188, 2003.

[5] Erdogan T.: Fiber grating spectra. J. Lightwave Technol., vol. 15, no. 8, pp. 1277-1294, 1997.

[6] Kashyap R.: Fiber Bragg gratings. San Diego Toronto, Academic Press, 1999.

Received: 06.05.2016 *Paper reviewed* *Accepted: 01.07.2016*

Aleksandra SIKORA, PhD, eng.

Graduated from the Faculty of Electrical Engineering, Automation and Informatics Kielce University of Technology in 2002. At the same Faculty received the PhD degree in electrical engineering in 2010. Main research interest: application of fiber Bragg gratings in measurement and telecommunication systems.

e-mail: a.sikora@tu.kielce.pl